Geophysical Research Letters®

RESEARCH LETTER
10.1029/2021GL093990

Key Points:

- Summer temperatures and the likelihood of heatwaves increase significantly over Korea and Japan in the positive Pacific-Japan (PJ) pattern
- Horizontal heat advection from the subtropical ocean is a key factor for the observed near-surface warming observed in Korea and Japan
- PJ-related near-surface circulation explains the intense warm advection

Supporting Information:

Supporting Information may be found in the online version of this article.

Correspondence to:

J. Kim,
joowan.k@gmail.com

Citation:

Noh, E., Kim, J., Jun, S.-Y., Cha, D.-H., Park, M.-S., Kim, J.-H., & Kim, H.-G. (2021). The role of the Pacific-Japan pattern in extreme heatwaves over Korea and Japan. *Geophysical Research Letters*, *48*, e2021GL093990. https://doi.org/10.1029/2021GL093990

Received 27 APR 2021
Accepted 3 SEP 2021

© 2021. American Geophysical Union. All Rights Reserved.

The Role of the Pacific-Japan Pattern in Extreme Heatwaves Over Korea and Japan

El Noh[1], Joowan Kim[1], Sang-Yoon Jun[2], Dong-Hyun Cha[3], Myung-Sook Park[4], Joo-Hong Kim[2], and Hyeong-Gyu Kim[1]

[1]Department of Atmospheric Sciences, Kongju National University, Gongju, South Korea, [2]Korea Polar Research Institute, Incheon, South Korea, [3]Ulsan National Institute of Science and Technology, Ulsan, South Korea, [4]Korea Institute of Ocean Science and Technology, Busan, South Korea

Abstract In the Northwestern Pacific, the meridionally propagating Rossby waves, known as the Pacific-Japan (PJ) pattern, is the dominant teleconnection pattern and is considered as a source of heatwaves in East Asia. In this study, the circulation and thermodynamic characteristics of these patterns were investigated based on daily timescale to evaluate their relationship with the likelihood of heatwaves in Korea and Japan. The investigations reveal that stations in Korea and Japan record approximately 90% increase in extremely hot days ($T_{max} > 35°C$) during the positive PJ pattern events. According to thermodynamic budget, horizontal heat advection is a key factor for the observed near-surface warming during the positive PJ. The circulation pattern during the positive PJ largely explains the enhanced warm advection and physical heating due to the increased insolation and adiabatic heating are secondary factors for near-surface warming. This phenomenon is robustly observed regardless of the definition.

Plain Language Summary In this study, the circulation and thermodynamic characteristics of these patterns were investigated based on daily timescale to evaluate their relationship with occurrence likelihood of heatwaves in Korea and Japan. The investigations reveal that stations in Korea and Japan record approximately 90% increase in extreme hot days during the positive PJ pattern events. According to thermodynamic budget calculations, horizontal heat advection is a key factor for the observed near-surface warming.

1. Introduction

The frequent heatwaves in recent decades account for significant socioeconomic problems in Korea and Japan. In Korea, record-breaking heatwaves were recorded in 2013, 2016, and 2018 and these were accompanied by many health and energy issues. In Japan, major heatwaves were also reported in 2013 along with consecutive 2018–2020, and there were associated with serious heat-related illnesses (Hayashida et al., 2019; Kang et al., 2020; Lim et al., 2019). In particular, the 2018 deadly heatwave was responsible for 42 deaths in Korea and 1,032 in Japan, with corresponding illnesses of more than 3,400 and 71,200, respectively (Imada et al., 2019; Iwasaki et al., 2019; Park & Chae, 2020). In general, heatwaves are accompanied by tropical nights, which are also lead to serious heat-related illnesses (Cinar et al., 2001; Park & Lee, 2006).

Because of the large detrimental impacts of heatwaves (e.g., W. Lee et al., 2018; Nakai et al., 1999), their characteristics and mechanisms have been extensively studied over Korea and Japan (Hong et al., 2018; Lee & Lee, 2016; Yeh et al., 2018; Yoon et al., 2020). According to many studies, the intensity and frequency of summer heatwaves are increasing globally (Christensen et al., 2013; Perkins & Alexander, 2013), with the recent increase of heatwaves frequency in East Asia partially attributed to anthropogenic activities (Imada et al., 2018; Shimpo et al., 2019). Considering that heatwaves are characterized by irregular interannual variation, their accurate prediction remains challenging. Consequently, many studies focus on the atmospheric circulations that are directly relevant to the occurrence of heatwaves (Lee & Lee, 2016; Shimpo et al., 2019; W. Wang et al., 2016, S. S. Y. Wang et al., 2019; Yeh et al., 2018; Yeo et al., 2019; Yoon et al., 2020).

The heatwaves, particularly reported in Korea and Japan, are generally related to the enhancement of the Northwestern Pacific Subtropical High (NPSH). During these heatwaves, the NPSH is largely modulated by the zonally propagating Rossby waves originating from Eurasia (Enomoto et al., 2003; Xu et al., 2019; Yeh et al., 2018; Yoon et al., 2020) and the meridionally propagating Rossby waves emanating from the

tropical western Pacific (He et al., 2018; Lee & Lee, 2016; Shimpo et al., 2019; S. S. Y. Wang et al., 2019; Yeo et al., 2019). The zonally propagating waves are often observed as synoptic-scale wave train connecting from Europe to East Asia. In spite of its scale, this is quasi-stationary because of the relatively slow westerly background in the summer, with its enhancement significantly modulating the NPSH and causing extreme events in East Asia (e.g., Coumou et al., 2018; Kornhuber et al., 2019; Shimpo et al., 2019; Xiang et al., 2013). The meridionally propagating waves are generally forced by deep convection in the western Pacific (near the Philippines) and propagate northward as thermally driven Rossby waves (Hoskins & Karoly, 1981; Sardeshmukh & Hoskins, 1988). The anticyclonic branch of these waves commonly overlaps the NPSH, thereby promoting its northwestward expansion. This process was advanced as a probable cause for the dangerous heatwaves in 2018 (Hsu et al., 2020; Shimpo et al., 2019). In addition, local sea surface temperature anomaly (Hasegawa et al., 2020; Wie et al., 2021) and midlatitude blocking (Yeh et al., 2018; Yoon et al., 2021) are known contributors to the heatwaves, although the latter can be considered as a part of the meridional waves.

These studies emphasize that the heatwaves in Korea and Japan are strongly coupled to the large-scale atmospheric circulation or teleconnection patterns. Among these patterns, the meridionally propagating Rossby waves, known as the Pacific-Japan (PJ) pattern have been investigated as a potential source of predictability in subseasonal and seasonal timescales (Guan et al., 2019; Kosaka et al., 2013; Kosaka & Nakamura, 2010; Nitta, 1987; Wakabayashi & Kawamura, 2004; Wang & Wang, 2018). Considering that the PJ pattern is forced by tropical convection over the Philippines and affects East Asia while it propagates northward, this pattern can be easily captured by 850-hPa geopotential difference at Taiwan and southern Japan (Kawamura & Ogasawara, 2006; Kubota et al., 2016; R. C. Y. Li et al., 2014; Nitta, 1987; Wakabayashi & Kawamura, 2004) and empirical orthogonal function (EOF) analysis over East Asia (Kosaka & Nakamura, 2006, 2008, 2010; Wu et al., 2016). They provide useful information for climate prediction of these regions.

The reported impacts of the PJ patterns in Korea and Japan are summarized as follows: (a) convection suppression, (b) high-pressure anomaly enhancement, (c) anticyclonic circulation promotion, and (d) enhancement of relatively warmer temperatures (Kosaka & Nakamura, 2006; Kubota et al., 2016). These characteristics generally produce hot and dry summers over the regions, including increased tropical cyclone activity over the South China Sea (Choi et al., 2010; Kubota et al., 2016). Recent studies also reported a significant relationship between positive PJ and East Asian heatwaves (Shimpo et al., 2019; Yeo et al., 2019; Yoon et al., 2020).

Despite the larger volume of studies, a clear physical feature connecting PJ and heatwaves is still limited, partially because the characteristics of the PJ pattern are commonly studied using monthly or climate time-scales. Based on daily analyses, we present that the near-surface warm advection is a key factor for the observed warm anomalies during positive PJ, which is one of potential causes of the Korea and Japan heatwaves.

Section 2 describes the data and methods used for the study. Section 3 summarizes important patterns of PJ in the daily timescale and provides thermodynamic features related to the warming. Last, a discussion is presented in Section 4.

2. Data and Methodology

2.1. Data

Hourly temperature data were obtained from the Hadley Centre Integrated Surface Database (HadISD; Dunn et al., 2016) and used for calculating maximum temperature (T_{max}) for the 40-year period from 1981 to 2020. The surface stations that provide hourly samples over Korea and Japan are used for the analysis. The primary data used for the pattern and budget analyses are the 6-hourly European Centre for Medium-Range Weather Forecasts (ECMWF) Re-Analysis version 5 (ERA-5; Hersbach et al., 2020) regridded into a 1.5° × 1.5° resolution. To reduce the high-frequency variability, a 5-day running average was applied for the time series, with all analyses focused on the boreal summer period (June-July-August [JJA]).

In order to characterize the atmospheric circulation related to the PJ pattern, the composite analysis was performed with respect to the central date of the PJ index defined by Equation 2 in Section 2.3. Anomaly fields were computed by removing daily climatologies that are defined for the period of 1981–2020.

2.2. Apparent Heat Source (Q1)

We calculated the atmospheric apparent heat source term (Q1) based on the thermodynamic energy equation. The thermodynamic equation and Q1 are related by the following equation (D.-K. Lee et al., 2008; Yanai et al., 1973):

$$\frac{dT}{dt} = -\vec{V} \cdot \nabla T + \left(\frac{p}{p_0}\right)^k \omega \frac{\partial \theta}{\partial p} + \frac{1}{c_p} Q_1 \tag{1}$$

where T, θ, $\vec{V}$, p, and ω are the temperature, potential temperature, horizontal wind vector, pressure, and vertical pressure velocity, respectively; ∇ denotes the horizontal gradient operator; and p_0 and c_p are the reference pressure (1000 hPa) and the specific heat of dry air at constant pressure, respectively. The calculated Q1 represents the total diabatic heating redistributed by unresolved mixing, which includes the radiative heating, latent heat release due to net condensation, and surface heat flux.

2.3. The PJ Index

Considering previous studies (Kubota et al., 2016; R. C. Y. Li et al., 2014; Wakabayashi & Kawamura, 2004), the PJ index in the present study was calculated by the difference of the normalized 850-hPa geopotential height anomaly between grid points in Taiwan (22°N, 120°E) and Japan (35°N, 140°E) as follows:

$$\text{PJ index} = \left[z^*\left(22°\text{N}, 120°\text{E}\right) - z^*\left(35°\text{N}, 140°\text{E}\right) \right] / 2 \tag{2}$$

where z* denotes the 850-hPa geopotential height anomaly normalized by the standard deviation of values for each grid point. This point-based PJ index is employed following Kubota et al. (2016) for comparison with previous studies. It is worth to note that it is almost identical to the one defined by EOF (Kubota et al., 2016), and overall results are independent of the definition.

This study will examine the evolution of PJ-related features through a composite analysis. The positive and negative events were selected based on ±1.0 standard deviation of the PJ index, respectively, while the peak was set as the central date (day 0). Finally, the indices that maintain the same phase must be at least 10 days apart to ensure the independence of the samples. Consequently, 31 positive and 34 negative events were obtained and used for subsequent analysis.

3. Result

3.1. Characteristics Observed

The heatwaves that occurred in Korea and Japan are closely related to the atmospheric circulation anomalies caused by the positive PJ pattern (e.g., Shimpo et al., 2019; Yeo et al., 2019). Figure 1 shows the distribution of T_{max} anomalies averaged for the positive and negative PJ pattern events. Depending on the phase of the PJ pattern, the T_{max} value for Korea and Japan varies considerably. In general, warming is observed in the data recorded in stations in the south part of Korea and Japan during the positive PJ pattern events, with the maximum value reaching approximately ~3°C (Figure 1a). The T_{max} difference is slightly lower during the negative PJ pattern events, with data for many stations in central and northern Japan indicating cooling (Figure 1b). These characteristics are clearly demonstrated by comparing the two T_{max} probability density functions relative to the phase of the PJ pattern (Figure 1c). The T_{max} distribution of the positive PJ pattern shifts to the warmer side and negatively skewed showing a significantly increased number of hot days. The number of days with T_{max} greater than 33°C, 35°C increased by approximately 250%, 90% during the positive PJ pattern, respectively. The T_{min} distribution of the positive PJ pattern also shifts to the warmer side (Figure S1). These surface observations ascertain that the likelihood of the heatwaves is clearly related to the PJ events.

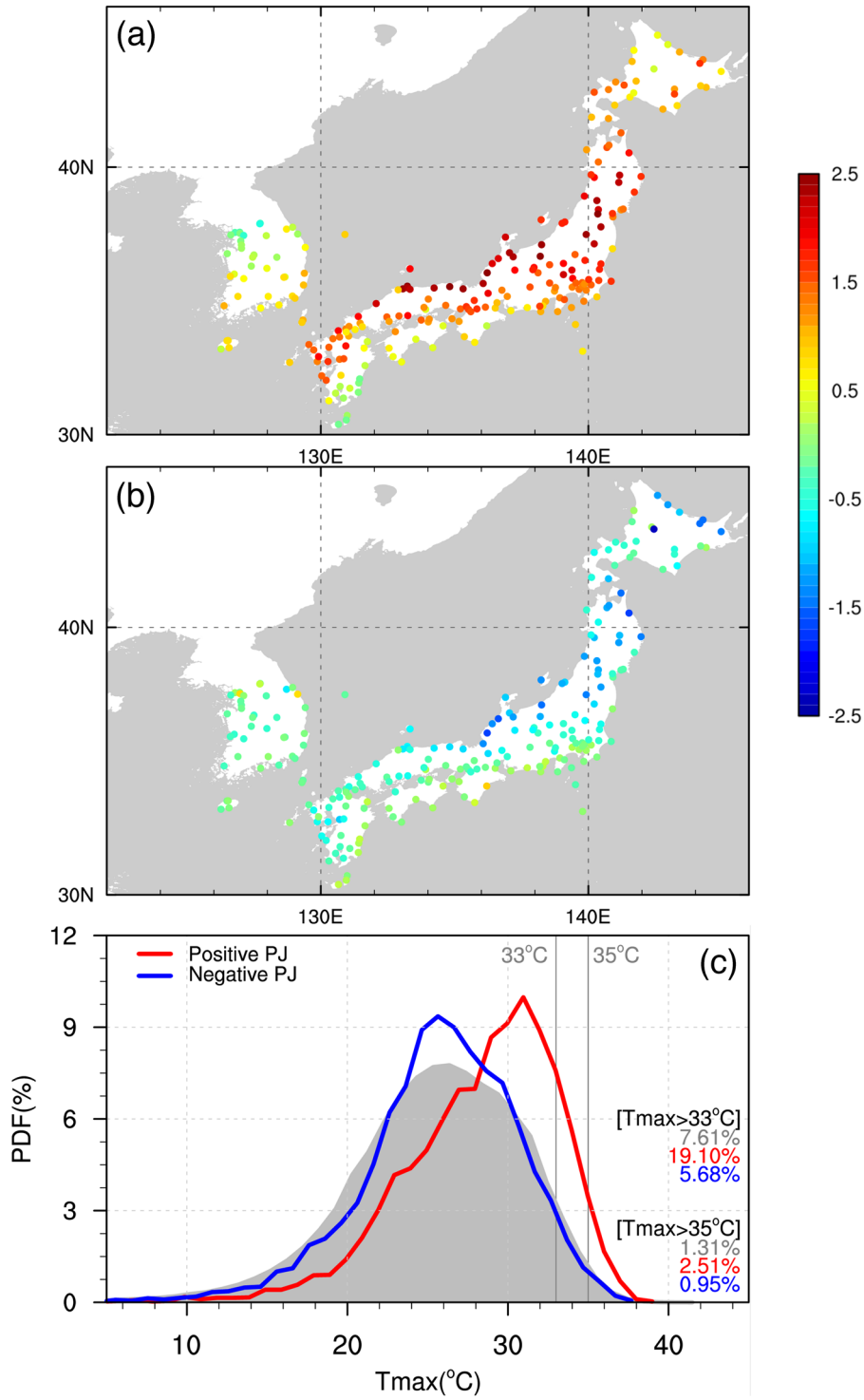

Figure 1. Composite daily maximum temperature anomaly (K) maps based on the (a) positive Pacific–Japan (PJ) index and (b) negative PJ index. (c) Plot of the probability density function versus T_{max} based on observation data for South Korea and Japan. The shaded area represents the entire data distribution, while the solid red line shows the positive PJ distribution and blue is the negative PJ distribution. The percentages assigned to each color highlights the probability that $T_{max} > 35$°C and $T_{max} > 33$°C.

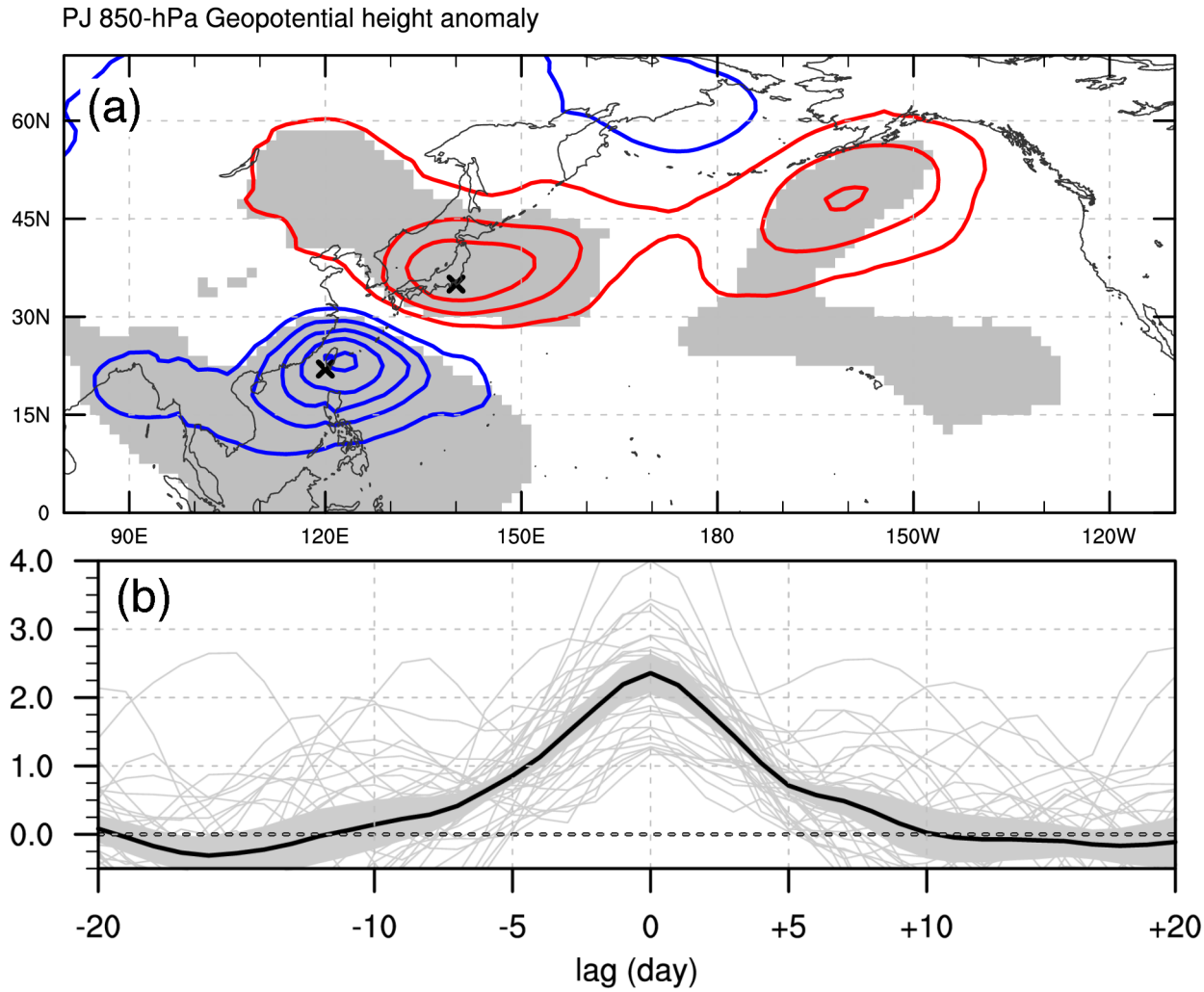

Figure 2. (a) Composite map of the 5-days running mean of the 850-hPa geopotential height anomaly of the positive Pacific–Japan (PJ) patterns. Contouring starts from ±10 m and the interval is 10 m, with zero lines omitted. The symbol "x" in (a) represent the locations stations in Taiwan and Japan in which data used for the PJ index were recorded. The shading highlights the statistically significant anomalies at the $p < 0.05$ level, determined using a two-tailed Student's *t*-test. (b) Normalized time series distribution of the positive PJ pattern index, with the gray line representing individual PJ indices, while the black line is the average, with the shaded portion indicating the 95% confidence interval of the mean.

The composite of the 850-hPa geopotential height for the positive PJ events (Figure 2a) presents a characteristic meridional dipole of low (cyclonic) and high pressure (anticyclonic) anomalies over the South China and Philippine seas and central Japan, respectively, which are consistent with previous studies (Kubota et al., 2016; Nitta, 1987). This pattern is obviously observed in the middle to lower troposphere (not shown) because of tropospheric propagation along the south westerly in the region (Kosaka & Nakamura, 2006). The daily timeseries of the PJ index (Figure 2b) shows that the PJ pattern evolves in a week or two, thereby providing enough time for propagation of the meridional Rossby waves and the associated atmospheric circulation. The spatial structure and time series of the PJ index during the negative PJ pattern events have similar characteristics except with an opposite sign (Figure S2). It is worth noting that the pattern further propagates and reaches southern Alaska and the west coast of North America. This feature is also reported in several studies (Kosaka & Nakamura, 2006; Nitta, 1987), although its impact on North America is not fully studied. The same dipole pattern (but with opposite phase) appears during the negative PJ events (Figure S3a).

This circulation pattern is coherent with other atmospheric and oceanic fields. Figure 3 shows composite anomalies for the daily surface air temperature (SAT), sea surface temperature (SST), total cloud cover, and

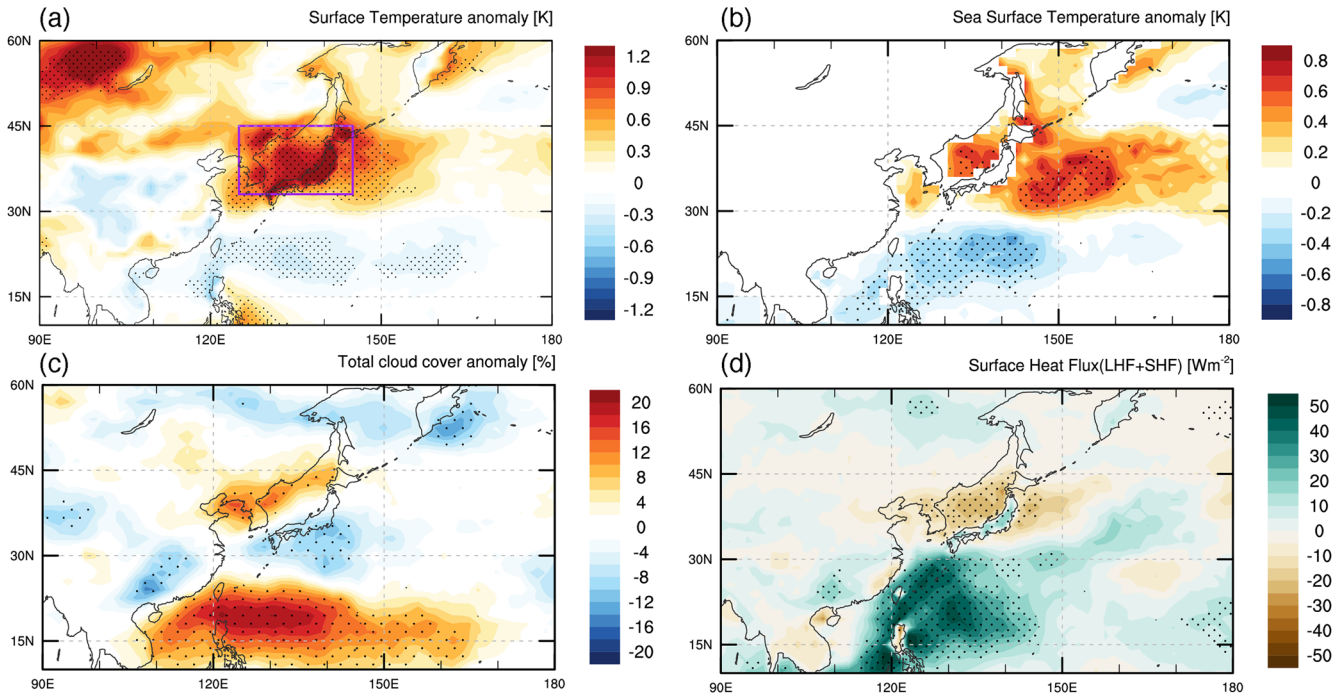

Figure 3. Composite maps showing the (a) surface temperature anomalies (K), (b) sea surface temperature anomalies (K), (c) total cloud cover anomalies (%), and (d) surface heat flux (latent heat flux + sensible heat flux) anomalies (Wm^{-2}) for the positive Pacific–Japan patterns. The dots highlight statistically significant anomalies at the $p < 0.05$ level, determined from the two-tailed Student's *t*-test.

surface heat flux for the 31 positive events. The composite anomalies of SAT show noticeable warming over Korea and Japan (Figure 3a), which consists well with the surface observations (Figure 1a). The SST anomaly also presents a similar warming pattern (Figure 3b), although it is further extended over the region of the Kuroshio extension implying the role of the ocean current. The surface heat flux from the ocean is also significantly reduced over the East Sea and east coast of Japan, likely due to the larger increase in the SAT compared to the SST (Figure 3d).

It is worth noting that the cloud cover is also reduced over southern Japan (Figure 3c) along with the insolation (Figure S4a). Due to the enhanced insolation, the land-surface temperature increases noticeably over Japan. This increase causes stronger heat fluxes from land (Figures S4b and S4c) deteriorating the heatwaves, while this mechanism is not found over ocean. The different responses of heat fluxes over land and ocean are related to the characteristics of the surface. It is also notable in the temperature budgets divided the surface type (Figure S5). The responses of cloud cover and insolation are different over Korea. This difference is related to an interaction with Changma front, which generally locates over this region.

This positive relationship between the midlatitude SAT and PJ has been reported in many studies (Kubota et al., 2016; Lee & Lee, 2016; Nitta, 1987; Wakabayashi & Kawamura, 2004). The warming over Korea and Japan is consistent with the high pressure (anticyclonic) anomaly observed in the region, and it has been explained as follows: (a) subsidence occurs due to the anticyclonic anomaly, (b) insolation increases because of cloud reduction, and (c) warm advection proceeds through southerlies (Kubota et al., 2016; Lee & Lee, 2016). In general, the results of this study are consistent with these explanations, however it is still not clear which one is the dominant process for the near-surface warming and potential cause of the heatwaves. It will be examined further using a thermodynamic budget in the subsequent section.

3.2. Cause of the Near-Surface Warming

The daily evolutions of the near-surface temperature are examined for the region where the midlatitude warming is significantly large (i.e., 33°–45°N and 125°–145°E; shown in the box with purple lines in Figure 3a). Overall, the SAT anomalies show positive and negative values near the central date of the positive

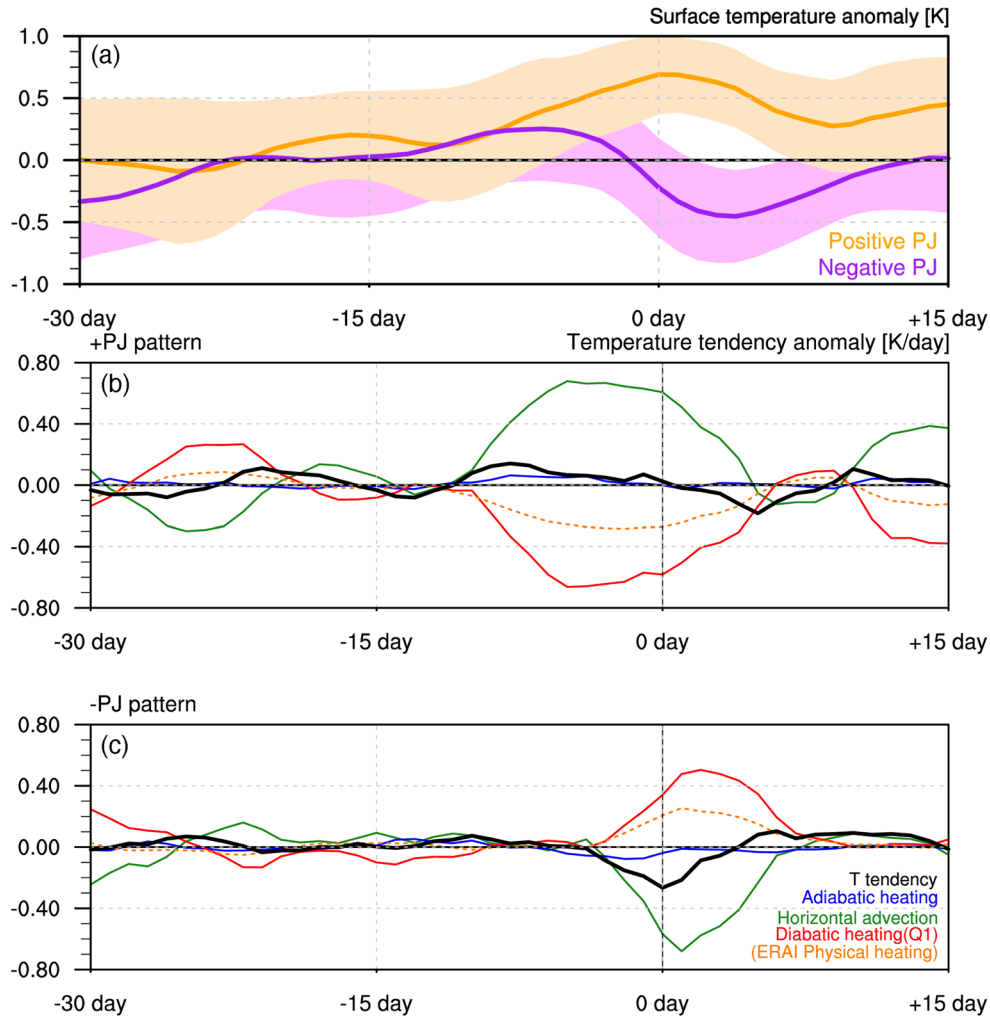

Figure 4. (a) Timeseries of the 5-days running mean surface temperature anomaly of each phase the Pacific–Japan (PJ) pattern from day −30 to day +15. The shading indicates the spread within ±0.5 standard deviations. (b and c) Temperature evolution of each phase of the PJ pattern based on a thermodynamic equation at 1000 hPa and the drivers, including the horizontal heat advection (thin green line), diabatic heating (Q1) (thin red line), and adiabatic heating (thin blue line). The thick black line represents the surface temperature trend anomaly, while the orange dashed line is for the ERA-Interim physical heating rate anomaly.

(yellow in Figure 4a) and negative (purple in Figure 4a) PJ pattern events, respectively. However, the anomaly persists longer with a stronger peak during the positive PJ pattern events compared to that of the negative PJ events. These results are also consistent with the surface observations (Figure 1), which exhibit stronger (asymmetric) temperature responses for the positive PJ patterns. The temperature data also presents a notable increase roughly 10 days before the central dates of the positive PJ patterns, and rapidly decreases several days before the central date for the negative PJ patterns.

The temperature tendency is further investigated using the thermodynamic equation (Figures 4b and 4c). The daily temperature tendency (black line) can be decomposed into the horizontal temperature advection (green line), adiabatic heating (blue line), and diabatic heating (red line) based on the calculated Q1 value. The most distinct feature is the large dominance of horizontal advection on the temperature tendency. Regarding the positive PJ patterns (Figure 4b), the surface temperature starts to increase significantly because of horizontal advection ~10 days before the central date. The adiabatic heating caused by subsidence also contributes to the heating, although this contribution is still secondary near the surface. Notably, the contribution of the subsidence-induced adiabatic warming is comparable to that of the horizontal advection above the ~850-hPa level (Figures S6 and S7); however the horizontal advection is the principal process

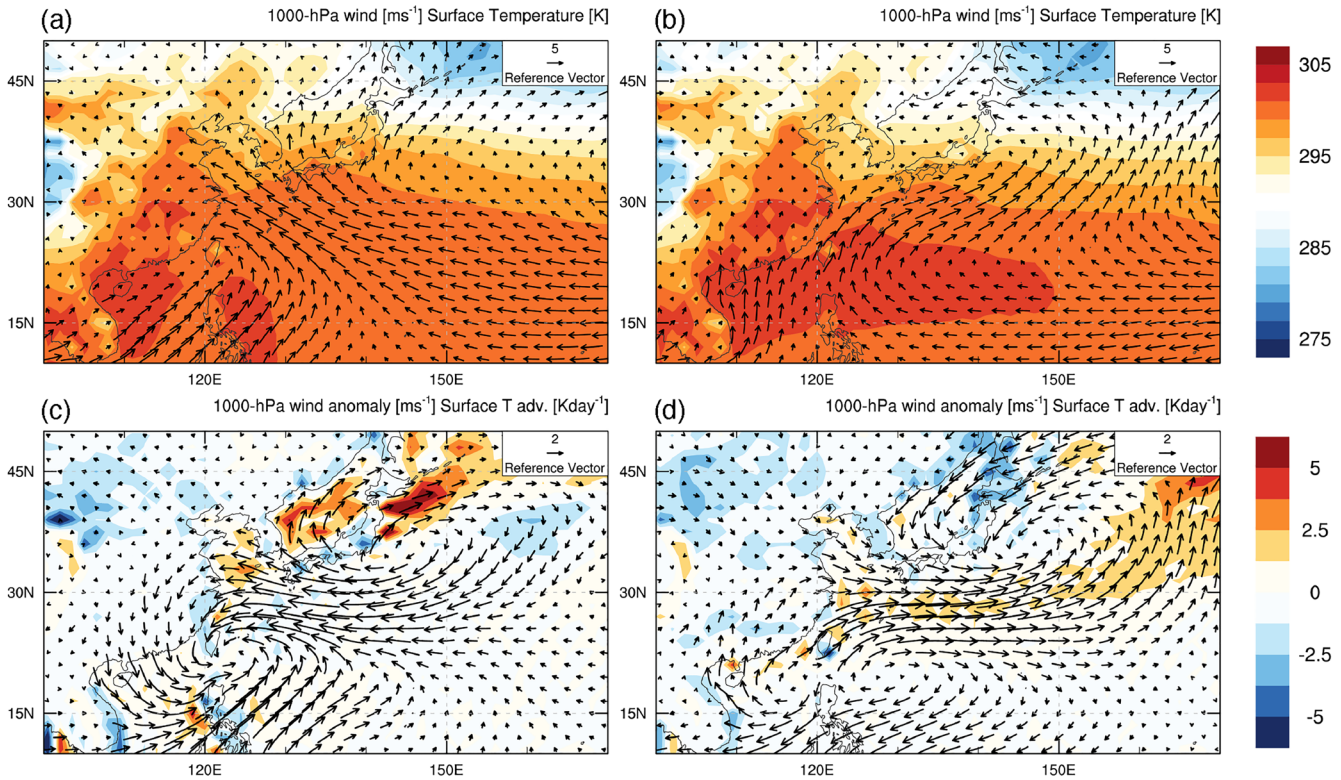

Figure 5. Composite maps involving the (a and b) surface temperature (shading, K) and horizontal wind at 1000-hPa (vector, ms^{-1}), and (c and d) horizontal advection of the surface temperature (shading, K day^{-1}) and horizontal wind anomalies at 1000-hPa (vector, ms^{-1}) for positive Pacific–Japan (PJ) patterns (left) and negative PJ patterns (right).

responsible for the near-surface warming. The Q1, which is a reasonable estimation of the physical heating and unresolved mixing process, offsets the warming tendency. This effect might be caused by outgoing longwave radiation, which increased due to near-surface warming. The total physical heating from the ERA-Interim also suggests that the net physical process adversely affects the observed warming during the positive PJ events. The negative PJ (Figure 4c) yield roughly the same interpretation, although their responses are stronger after the central date. These characteristics are generally similar for the EOF-based PJ definition (Figure S8). The westerly dominates over Japan (still crossing the isotherms), and the temperature advection is slightly stronger for the negative PJ. However, the temperature advection is still the primary factor for the temperature tendency.

Increased insolation due to cloud reduction is considered a major process that can explain the observed warming in Korea and Japan (e.g., Kosaka & Nakamura, 2006; Tao et al., 2017; Wakabayashi & Kawamura, 2004). In fact, the reduced cloud cover amount (Figure 2c) and increased land-surface flux over Japan are supportive of this idea (Figures S4b and S4c). However, warming by these processes is weak compared to that associated with the horizontal advection, and these processes are too localized to drive the regional-scale warming observed during the positive PJ pattern events. For example, the same processes are not observed over Korea and the East Sea, where significant warming is still observed.

The details of horizontal advection are examined to better understand the role of the PJ-related circulation on horizontal temperature advection. The near-surface temperature fields show a large gradient over Korea and Japan for the positive and negative PJ patterns (Figure 5), which represents a seasonal characteristic of both regions. However, the circulation fields differ notably between the positive and negative events. The southeasterly dominates over the East China Sea and southern Japan for the positive PJ pattern events, inducing intense warm advection over Korea and Japan by crossing the temperature gradient in the regions (Figure 5a). On the other hand, the southwesterly, characterized by parallels isotherms, prevails over the regions but induces no significant temperature advection for the negative PJ patterns.

This feature is more pronounced in the PJ-related anomalies (Figures 5c and 5d). For positive PJ, the near-surface winds show a clear dipole of cyclone and anticyclone, respectively over the subtropical and midlatitude regions of the western Pacific. This circulation pattern induces southeasterlies between the dipoles, thereby enhancing heat and moisture transports from the subtropical ocean toward Korea and Japan, whereas negative PJ patterns inhibit such transport by preventing westerlies. This surface circulation evolves as a part of the meridionally propagating Rossby waves under the background of the Asian summer monsoon and subtropical high (Kosaka & Nakamura, 2006, 2010). The time-lag composite of the circulation fields (Figures S9 and S10) demonstrates that this response can evolve roughly in a weekly timescale, which corresponds to the energy propagation duration of Rossby waves. The time lag in the temperature tendency during the negative PJ pattern is likely related to this energy propagation. In fact, the cold advection during negative PJ originates from the Okhotsk Sea (Figure 5d), which locates far north of the warm advection during positive PJ (Figures S9 and S10).

4. Conclusion

In this study, the evolution of the PJ pattern and surface temperature on an intraseasonal timescale were detailly examined. The PJ pattern is one of the most dominant teleconnection patterns in the western North Pacific during the boreal summer. The analysis based on 40 years of ERA5 and surface station data confirms that the daily PJ index and corresponding Rossby wave pattern are strongly related to the summer climate over Korea and Japan. In particular, the subtropical-to-midlatitude dipole pattern and balanced near-surface circulation play prominent roles over the western North Pacific.

Summer temperatures over Korea and Japan are significantly affected by positive PJ patterns, and the likelihood of heatwaves is also significantly increased with the event. The thermodynamic budget analysis on a daily timescale revealed the horizontal advection of heat by southeasterly winds as the principal factor responsible for elevated near-surface temperatures over Korea and Japan. The dipole patterns developed over the subtropics and midlatitude as a part of the PJ-related Rossby waves account for the southeasterlies and warm advection. During the positive PJ events, a high-pressure system develops over Japan, which aggravates the near-surface warming through subsidence and additional insolation, although these impacts turn out to be secondary factors. These results are robust regardless of the PJ definition, which can slightly modifies the Rossby wave pattern.

It is worth noting that positive PJ patterns are also likely related to coastal marine heatwaves (see Figure 3b), which have devastating impacts on aquaculture and fisheries (S. Lee et al., 2020; Y. Li et al., 2019; Oliver et al., 2018). Therefore, atmospheric and marine heatwaves can interact through atmosphere-ocean coupling processes such as the heat flux exchange (e.g., Olita et al., 2007; Figure 3d). The frequency and intensity of atmospheric (Christensen et al., 2013; Perkins & Alexander, 2013) and marine heatwaves are increasing (Frölicher & Laufkötter, 2018; Oliver et al., 2018) due to global warming and the associated circulation changes (Coumou et al., 2018; Mann et al., 2017). However, their physical mechanisms are not clearly understood, and the predictability of the heatwaves is generally low (Olita et al., 2006, 2007; Sparnocchia et al., 2006). Several studies suggest that the PJ pattern is an important source of predictability over the East Asian region (Kosaka et al., 2012, 2013; Wu et al., 2016; Xie et al., 2009). The PJ pattern is generally forced by deep convection in the western Pacific (near the Philippines) and propagates poleward as thermally driven Rossby waves (Hoskins & Karoly, 1981; Sardeshmukh & Hoskins, 1988). Detailed understanding on the pattern and other heatwave-related atmosphere-ocean coupled modes would enhance the prediction of heatwave in subseasonal to seasonal timescale. In addition to the PJ pattern, the recently emerging meridional wave train phenomenon (Kornhuber et al., 2017, 2019; Petoukhov et al., 2013; Yoon et al., 2020) is another important process that requires further investigation.

Data Availability Statement

Copernicus Climate Change Service (C3S) (2017): ERA5: Fifth generation of ECMWF atmospheric reanalyses of the global climate. Copernicus Climate Change Service Climate Data Store (CDS), date of access. https://cds.climate.copernicus.eu/cdsapp#!/home. Met Office Hadley Centre; National Centers for Environmental Information—NOAA (2020): HadISD: Global sub-daily, surface meteorological station data,

1931–2019, v3.1.0.2019f. Centre for Environmental Data Analysis, date of citation. https://catalogue.ceda.ac.uk/uuid/e488dccd09e1446d90978b75036475e2.

Acknowledgments
This work was funded by the Korea Meteorological Administration Research and Development Program under Grant KMI(KMI2020-01412). This work was funded by the Ministry of Oceans and Fisheries, Korea project, entitled "Investigation and Prediction System Development of Marine Heatwave around the Korean Peninsula originated from the Sub-Arctic and Western Pacific" (20190344).

References

Choi, K.-S., Wu, C.-C., & Cha, E.-J. (2010). Change of tropical cyclone activity by Pacific-Japan teleconnection pattern in the western North Pacific. *Journal of Geophysical Research*, *115*(D19), D19114. https://doi.org/10.1029/2010JD013866

Christensen, J. H., Krishna Kumar, K., Aldrian, E., An, S.-I., Cavalcanti, I. F. A., de Castro, M., et al. (2013). Climate phenomena and their relevance for future regional climate change. In *Climate Change 2013: The physical science basis. Contribution of working group I to the fifth assessment report of the intergovernmental panel on climate change*. http://www.climatechange2013.org/images/report/WG1AR5_FOD_Ch14_All_Final.pdf

Çinar, Y., Şenyol, A. M., & Duman, K. (2001). Blood viscosity and blood pressure: Role of temperature and hyperglycemia. *American Journal of Hypertension*, *14*(5), 433–438. https://doi.org/10.1016/S0895-7061(00)01260-7

Coumou, D., Di Capua, G., Vavrus, S., Wang, L., & Wang, S. (2018). The influence of Arctic amplification on mid-latitude summer circulation. *Nature Communications*, *9*(1), 2959. https://doi.org/10.1038/s41467-018-05256-8

Dunn, R. J. H., Willett, K. M., Parker, D. E., & Mitchell, L. (2016). Expanding HadISD: Quality-controlled, sub-daily station data from 1931. *Geoscientific Instrumentation, Methods and Data Systems*, *5*(2), 473–491. https://doi.org/10.5194/gi-5-473-2016

Enomoto, T., Hoskins, B. J., & Matsuda, Y. (2003). The formation mechanism of the Bonin high in August. *Quarterly Journal of the Royal Meteorological Society*, *129*(587), 157–178. https://doi.org/10.1256/qj.01.211

Frölicher, T. L., & Laufkötter, C. (2018). Emerging risks from marine heat waves. *Nature Communications*, *9*(1), 650. https://doi.org/10.1038/s41467-018-03163-6

Guan, W. N., Hu, H. B., Ren, X. J., & Yang, X. Q. (2019). Subseasonal zonal variability of the western Pacific subtropical high in summer: Climate impacts and underlying mechanisms. *Climate Dynamics*, *53*(5–6), 3325–3344. https://doi.org/10.1007/s00382-019-04705-4

Hasegawa, A., Imada, Y., Shiogama, H., Mori, M., Tatebe, H., & Watanabe, M. (2020). Impact of air–sea coupling on the probability of occurrence of heat waves in Japan. *Progress in Earth and Planetary Science*, *7*(1). https://doi.org/10.1186/s40645-020-00390-8

Hayashida, K., Shimizu, K., & Yokota, H. (2019). Severe heatwave in Japan. *Acute Medicine & Surgery*, *6*(2), 206–207. https://doi.org/10.1002/ams2.387

He, C., Lin, A., Gu, D., Li, C., Zheng, B., Wu, B., & Zhou, T. (2018). Using eddy geopotential height to measure the western North Pacific subtropical high in a warming climate. *Theoretical and Applied Climatology*, *131*(1–2), 681–691. https://doi.org/10.1007/s00704-016-2001-9

Hersbach, H., Bell, B., Berrisford, P., Hirahara, S., Horányi, A., Muñoz-Sabater, J., et al. (2020). The ERA5 global reanalysis. *Quarterly Journal of the Royal Meteorological Society*, *146*(730), 1999–2049. https://doi.org/10.1002/qj.3803

Hong, J. S., Yeh, S. W., & Seo, K. H. (2018). Diagnosing physical mechanisms leading to pure heat waves versus pure tropical nights over the Korean Peninsula. *Journal of Geophysical Research: Atmospheres*, *123*(14), 7149–7160. https://doi.org/10.1029/2018JD028360

Hoskins, B. J., & Karoly, D. J. (1981). The steady linear response of a spherical atmosphere to thermal and orographic forcing. *Journal of the Atmospheric Sciences*, *38*(6), 1179–1196. https://doi.org/10.1175/1520-0469(1981)038.1179:TSLROA.2.0.CO;2

Hsu, P. C., Qian, Y., Liu, Y., Murakami, H., & Gao, Y. (2020). Role of abnormally enhanced MJO over the western pacific in the formation and subseasonal predictability of the record-breaking northeast Asian heatwave in the summer of 2018. *Journal of Climate*, *33*(8), 3333–3349. https://doi.org/10.1175/JCLI-D-19-0337.1

Imada, Y., Shiogama, H., Takahashi, C., Watanabe, M., Mori, M., Kamae, Y., & Maeda, S. (2018). Climate change increased the likelihood of the 2016 heat extremes in Asia. *Bulletin of the American Meteorological Society*, *99*(1), S97–S101. https://doi.org/10.1175/BAMS-D-17-0109.1

Imada, Y., Watanabe, M., Kawase, H., Shiogama, H., & Arai, M. (2019). The July 2018 high temperature event in Japan could not have happened without human-induced global warming. *SOLA*, *15A*(A), 8–12. https://doi.org/10.2151/sola.15A-002

Iwasaki, Y., KasaiHirukawa, K. K., & Kawakami, M. (2019). The impact of Japan heatwave on community emergency medicine in 2018. *Prehospital and Disaster Medicine*, *34*(s3), s29–s20. https://doi.org/10.1017/S1049023X1900076110.1017/s1049023x19000785

Kang, C., Park, C., Lee, W., Pehlivan, N., Choi, M., Jang, J., & Kim, H. (2020). Heatwave-related mortality risk and the risk-based definition of heat wave in South Korea: A nationwide time-series study for 2011–2017. *International Journal of Environmental Research and Public Health*, *17*(16), 1–12. https://doi.org/10.3390/ijerph17165720

Kawamura, R., & Ogasawara, T. (2006). On the role of typhoons in generating PJ teleconnection patterns over the western North Pacific in late summer. *SOLA*, *2*, 37–40.

Kornhuber, K., Osprey, S., Coumou, D., Petri, S., Petoukhov, V., Rahmstorf, S., & Gray, L. (2019). Extreme weather events in early summer 2018 connected by a recurrent hemispheric wave-7 pattern. *Environmental Research Letters*, *14*(5), 054002. https://doi.org/10.1088/1748-9326/ab13bf

Kornhuber, K., Petoukhov, V., Petri, S., Rahmstorf, S., & Coumou, D. (2017). Evidence for wave resonance as a key mechanism for generating high-amplitude quasi-stationary waves in boreal summer. *Climate Dynamics*, *49*(5–6), 1961–1979. https://doi.org/10.1007/s00382-016-3399-6

Kosaka, Y., Chowdary, J. S., Xie, S. P., Min, Y. M., & Lee, J. Y. (2012). Limitations of seasonal predictability for summer climate over East Asia and the Northwestern Pacific. *Journal of Climate*, *25*(21), 7574–7589. https://doi.org/10.1175/JCLI-D-12-00009.1

Kosaka, Y., & Nakamura, H. (2006). Structure and dynamics of the summertime Pacific–Japan teleconnection pattern. *Quarterly Journal of the Royal Meteorological Society*, *132*(619), 2009–2030. https://doi.org/10.1256/qj.05.204

Kosaka, Y., & Nakamura, H. (2008). A comparative study on the dynamics of the Pacific-Japan (PJ) teleconnection pattern based on reanalysis datasets. *Sola*, *4*, 9–12.

Kosaka, Y., & Nakamura, H. (2010). Mechanisms of meridional teleconnection observed between a summer monsoon system and a subtropical anticyclone. Part I: The Pacific-Japan pattern. *Journal of Climate*, *23*(19), 5085–5108. https://doi.org/10.1175/2010JCLI3413.1

Kosaka, Y., Xie, S. P., Lau, N. C., & Vecchi, G. A. (2013). Origin of seasonal predictability for summer climate over the Northwestern Pacific. *Proceedings of the National Academy of Sciences of the United States of America*, *110*(19), 7574–7579. https://doi.org/10.1073/pnas.1215582110

Kubota, H., Kosaka, Y., & Xie, S. (2016). A 117-year long index of the Pacific-Japan pattern with application to interdecadal variability. *International Journal of Climatology*, *36*(4), 1575–1589. https://doi.org/10.1002/joc.4441

Lee, D.-K., Park, J.-G., & Kim, J.-W. (2008). Heavy rainfall events lasting 18 days from July 31 to August 17, 1998, over Korea. *Journal of the Meteorological Society of Japan*, *86*(2), 313–333. https://doi.org/10.2151/jmsj.86.313
Lee, S., Park, M.-S., Kwon, M., Kim, Y. H., & Park, Y.-G. (2020). Two major modes of East Asian marine heatwaves. *Environmental Research Letters*, *15*(7), 074008. https://doi.org/10.1088/1748-9326/ab8527
Lee, W., Choi, H. M., Lee, J. Y., Kim, D. H., Honda, Y., & Kim, H. (2018). Temporal changes in mortality impacts of heat wave and cold spell in Korea and Japan. *Environment International*, *116*, 136–146. https://doi.org/10.1016/j.envint.2018.04.017
Lee, W., & Lee, M. (2016). Interannual variability of heat waves in South Korea and their connection with large-scale atmospheric circulation patterns. *International Journal of Climatology*, *36*(15), 4815–4830. https://doi.org/10.1002/joc.4671
Li, R. C. Y., Zhou, W., & Li, T. (2014). Influences of the Pacific–Japan Teleconnection Pattern on Synoptic-Scale Variability in the Western North Pacific. *Journal of Climate*, *27*(1), 140–154. https://doi.org/10.1175/JCLI-D-13-00183.1
Li, Y., Ren, G., Wang, Q., & You, Q. (2019). More extreme marine heatwaves in the China Seas during the global warming hiatus. *Environmental Research Letters*, *14*(10), 104010. https://doi.org/10.1088/1748-9326/ab28bc
Lim, Y. H., Lee, K. S., Bae, H. J., Kim, D., Yoo, H., Park, S., & Hong, Y. C. (2019). Estimation of heat-related deaths during heat wave episodes in South Korea (2006–2017). *International Journal of Biometeorology*, *63*(12), 1621–1629. https://doi.org/10.1007/s00484-019-01774-2
Mann, M. E., Rahmstorf, S., Kornhuber, K., Steinman, B. A., Miller, S. K., & Coumou, D. (2017). Influence of anthropogenic climate change on planetary wave resonance and extreme weather events. *Scientific Reports*, *7*. https://doi.org/10.1038/srep45242
Nakai, S., Itoh, T., & Morimoto, T. (1999). Deaths from heat-stroke in Japan: 1968–1994. *International Journal of Biometeorology*, *43*(3), 0124. https://doi.org/10.1007/s004840050127
Nitta, T. (1987). Convective activities in the Tropical Western Pacific and their impact on the Northern Hemisphere Summer Circulation. *Journal of the Meteorological Society of Japan. Series II*, *65*(3), 373–390. https://doi.org/10.2151/jmsj1965.65.3_373
Olita, A., Sorgente, R., Natale, S., Gaberšek, S., Ribotti, A., Bonanno, A., & Patti, B. (2007). Effects of the 2003 European heatwave on the Central Mediterranean Sea: Surface fluxes and the dynamical response. *Ocean Science*, *3*(2), 273–289. https://doi.org/10.5194/os-3-273-2007
Olita, A., Sorgente, R., Ribotti, A., Natale, S., & Gaber, S. (2006). Effects of the 2003 European heatwave on the Central Mediterranean Sea surface layer: A numerical simulation. *Ocean Science*, *3*(3), 85–125. https://doi.org/10.5194/osd-3-85-2006
Oliver, E. C. J., Donat, M. G., Burrows, M. T., Moore, P. J., Smale, D. A., Alexander, L. V., et al. (2018). Longer and more frequent marine heatwaves over the past century. *Nature Communications*, *9*(1), 1324. https://doi.org/10.1038/s41467-018-03732-9
Park, J. & Chae, Y. (2020). Analysis of heat-related illness and excess mortality by heat waves in South Korea in 2018. *Journal of the Korean Geographical Society*, *55*(4), 391–408. https://doi.org/10.22776/kgs.2020.55.4.391
Park, J. K., & Lee, D. G. (2006). Correlation between daily mortality and temperature of Seoul in summer. In *99th Annual Meeting of Air and Waste Management Association*. New Orleans, LA.
Perkins, S. E., & Alexander, L. V. (2013). On the measurement of heat waves. *Journal of Climate*, *26*(13), 4500–4517. https://doi.org/10.1175/JCLI-D-12-00383.1
Petoukhov, V., Rahmstorf, S., Petri, S., & Schellnhuber, H. J. (2013). Quasiresonant amplification of planetary waves and recent Northern Hemisphere weather extremes. *Proceedings of the National Academy of Sciences*, *110*(14), 5336–5341. https://doi.org/10.1073/pnas.1222000110
Sardeshmukh, P. D., & Hoskins, B. J. (1988). The generation of global rotational flow by steady idealized tropical divergence. *Journal of the Atmospheric Sciences*, *45*(7), 1228–1251. https://doi.org/10.1175/1520-0469(1988)045<1228:TGOGRF.2.0.CO;2
Shimpo, A., Takemura, K., Wakamatsu, S., Togawa, H., Mochizuki, Y., Takekawa, M., et al. (2019). Primary factors behind the heavy rain event of July 2018 and the subsequent heat wave in Japan. *SOLA*, *15A*(A), 13–18. https://doi.org/10.2151/sola.15A-003
Sparnocchia, S., Schiano, M. E., Picco, P., Bozzano, R., & Cappelletti, A. (2006). The anomalous warming of summer 2003 in the surface layer of the Central Ligurian Sea (Western Mediterranean). *Annales Geophysicae*, *24*(2), 443–452. https://doi.org/10.5194/angeo-24-443-2006
Tao, L., Li, T., Ke, Y.-H., & Zhao, J.-W. (2017). Causes of interannual and interdecadal variations of the summertime Pacific–Japan-like pattern over East Asia. *Journal of Climate*, *30*(22), 8845–8864. https://doi.org/10.1175/JCLI-D-15-0817.1
Wakabayashi, S., & Kawamura, R. (2004). Extraction of major teleconnection patterns possibly associated with the anomalous summer climate in Japan. *Journal of the Meteorological Society of Japan*, *82*(6), 1577–1588. https://doi.org/10.2151/jmsj.82.1577
Wang, C., & Wang, L. (2018). Combined effects of synoptic-scale teleconnection patterns on summer precipitation in Southern China. *Atmosphere*, *9*(4), 154. https://doi.org/10.3390/atmos9040154
Wang, S. S. Y., Kim, H., Coumou, D., Yoon, J., Zhao, L., & Gillies, R. R. (2019). Consecutive extreme flooding and heat wave in Japan: Are they becoming a norm? *Atmospheric Science Letters*, *20*(10), 2–5. https://doi.org/10.1002/asl.933
Wang, W., Zhou, W., Li, X., Wang, X., & Wang, D. (2016). Synoptic-scale characteristics and atmospheric controls of summer heat waves in China. *Climate Dynamics*, *46*(9–10), 2923–2941. https://doi.org/10.1007/s00382-015-2741-8
Wie, J., Moon, B.-K., Hyun, Y.-K., & Lee, J. (2021). Impact of local atmospheric circulation and sea surface temperature of the East Sea (Sea of Japan) on heat waves over the Korean Peninsula. *Theoretical and Applied Climatology*, *144*, 431–446. https://doi.org/10.1007/s00704-021-03546-8
Wu, B., Zhou, T., & Li, T. (2016). Impacts of the Pacific–Japan and circumglobal teleconnection patterns on the interdecadal variability of the East Asian Summer Monsoon. *Journal of Climate*, *29*(9), 3253–3271. https://doi.org/10.1175/JCLI-D-15-0105.1
Xiang, B., Wang, B., Yu, W., & Xu, S. (2013). How can anomalous western North Pacific Subtropical High intensify in late summer? *Geophysical Research Letters*, *40*(10), 2349–2354. https://doi.org/10.1002/grl.50431
Xie, S.-P., Hu, K., Hafner, J., Tokinaga, H., Du, Y., Huang, G., & Sampe, T. (2009). Indian Ocean capacitor effect on Indo–Western Pacific climate during the summer following El Niño. *Journal of Climate*, *22*(3), 730–747. https://doi.org/10.1175/2008JCLI2544.1
Xu, P., Wang, L., Chen, W., Feng, J., & Liu, Y. (2019). Structural changes in the Pacific-Japan pattern in the late 1990s. *Journal of Climate*, *32*(2), 607–621. https://doi.org/10.1175/JCLI-D-18-0123.1
Yanai, M., Esbensen, S., & Chu, J.-H. (1973). Determination of bulk properties of tropical cloud clusters from large-scale heat and moisture budgets. *Journal of the Atmospheric Sciences*, *30*(4), 611–627. https://doi.org/10.1175/1520-0469(1973)030.0611:DOBPOT.2.0.CO;2
Yeh, S.-W., Won, Y.-J., Hong, J.-S., Lee, K.-J., Kwon, M., Seo, K.-H., & Ham, Y.-G. (2018). The record-breaking heat wave in 2016 over South Korea and its physical mechanism. *Monthly Weather Review*, *146*(5), 1463–1474. https://doi.org/10.1175/MWR-D-17-0205.1
Yeo, S. R., Yeh, S. W., & Lee, W. S. (2019). Two Types of heat wave in Korea associated with atmospheric circulation pattern. *Journal of Geophysical Research: Atmospheres*, *124*(14), 7498–7511. https://doi.org/10.1029/2018JD030170

Yoon, D., Cha, D.-H., Lee, M.-I., Min, K.-H., Jun, S.-Y., & Choi, Y. (2021). Comparison of regional climate model performances for different types of heat waves over South Korea. *Journal of Climate*, *34*(6), 2157–2174. https://doi.org/10.1175/JCLI-D-20-0422.1

Yoon, D., Cha, D.-H., Lee, M.-I., Min, K.-H., Kim, J., Jun, S.-Y., & Choi, Y. (2020). Recent changes in heatwave characteristics over Korea. *Climate Dynamics*, *55*(7–8), 1685–1696. https://doi.org/10.1007/s00382-020-05420-1